EFDA–JET–CP(09)06/14

P.C. de Vries, Y. Sakamoto, X. Litaudon, M.N.A. Beurskens, M. Brix, K. Crombé, T. Fujita, C. Giroud, N.C. Hawkes, N. Hayashi, E. Joffrin, P. Mantica, G. Matsunaga, N. Oyama, V. Parail, A. Salmi, K. Shinohara, D. Strintzi, T. Suzuki, M. Takechi, H. Takenaga, T. Tala, M. Tsalas, H. Urano, I. Voitsekhovitch, M. Yoshida, the JT-60 team and JET EFDA contributors

Identity Physics Experiment on Internal Transport Barriers in JT-60U and JET

Identity Physics Experiment on Internal Transport Barriers in JT-60U and JET

P.C. de Vries[1], Y. Sakamoto[2], X. Litaudon[3], M.N.A. Beurskens[1], M. Brix[1], K. Crombé[4], T. Fujita[2], C. Giroud[1], N.C. Hawkes[1], N. Hayashi[2], E. Joffrin[3], P. Mantica[5], G. Matsunaga[2], N. Oyama[2], V. Parail[1], A. Salmi[6], K. Shinohara[2], D. Strintzi[7], T. Suzuki[2], M. Takechi[2], H. Takenaga[2], T. Tala[8], M. Tsalas[9], H. Urano[2], I. Voitsekhovitch[1], M. Yoshida[2], the JT-60 team[+] and JET EFDA contributors*

JET-EFDA, Culham Science Centre, OX14 3DB, Abingdon, UK

[1]EURATOM-UKAEA Fusion Association, Culham Science Centre, OX14 3DB, Abingdon, OXON, UK
[2]Japan Atomic Energy Agency, Naka, Ibaraki-ken 311-0193, Japan
[3]CEA, IRFM, F-13108 St-Paul-Lez-Durance, France
[4]Department of Applied Physics, Ghent University, Rozier 44, 9000 Gent, Belgium
[5]Istituto di Fisica del Plasma, EURATOM/ENEA-CNR Association, Milano, Italy
[6]Association Euratom-Tekes, Helsinki University of Technology, P.O. Box 4100, Finland
[7]National Technical University of Athens, EURATOM Association, GR-15773, Athens
[8]Association Euratom-Tekes, VTT, PO Box 1000, 02044 VTT, Finland
[9]Association EURATOM-Hellenic Republic, NCSR Demokritos, Attica, Greece
[+]See annex of N. Oyama et al
(Proc. 22 [nd] IAEA Fusion Energy Conference, Geneva, Switzerland (2008)).
** See annex of F. Romanelli et al, "Overview of JET Results",*
(Proc. 22 [nd] IAEA Fusion Energy Conference, Geneva, Switzerland (2008)).

Preprint of Paper to be submitted for publication in Proceedings of the
36th EPS Conference on Plasma Physics, Sofia, Bulgaria.
(29th June 2009 - 3rd July 2009)

ABSTRACT.
A series of experiments have been carried out in 2008 at JT-60U and JET in order to find common characteristics and differences in Internal Transport Barriers (ITBs) observed. The identity experiments succeeded in matching the profiles of most dimensionless parameters at the time ITBs were triggered. Thereafter the q-profile development deviated due to differences in non-inductive current profile, affecting the ITB. Furthermore, the ITBs in JET were found to be more strongly influenced by the H-mode or ELM conditions. It was found to be more difficult to match the plasma rotation characteristics in both devices. However, the wide range of Mach number obtained in these experiments showed to have little effect on the triggering of ITBs in plasmas with reversed magnetic shear. But the toroidal rotation and more specifically the rotational shear had an impact on the subsequent growth and allowed the formation of strong ITBs.

1. INTRODUCTION

Internal transport barriers or ITBs in fusion plasmas are an intriguing phenomenon, where turbulence driven transport is locally reduced, causing an improvement in the confinement properties [1, 2]. Internal transport barriers are considered as a possible way to enhance the energy confinement in Advanced Tokamak scenarios that aim to provide fully non-inductive operation of ITER at moderate plasma current but high pressures [3-5]. But the study of transport barriers may also give insight in the physics of turbulence and transport in fusion plasmas in general.

Similarities but also noted variations between ITBs in various devices have been reported [6]. Different physical mechanisms are thought to enable the formation of transport barriers. The mechanism in one device may differ from that in others, making a comparison of observations not always easy. Hence, for the first time a series of experiments have been carried out at JT-60U and JET in order to find common characteristics and differences in the process of ITB formation, with the aim to improve the understanding of the physics behind the triggering and sustainement of transport barriers.

Earlier comparisons between JT-60U and JET have highlighted the differences with respect to the Toroidal Field (TF) ripple and its impact on the H-mode pedestal and plasma rotation [7,8]. The question arises if such differences will affect internal transport barriers too. A strong H-mode pedestal and large Edge Localised Modes (ELMs) in JET usually have a significantly degrading influence on ITBs and the mechanism for this effect is not well understood [9]. Similarly, ELMs have been reported to affect ITBs in JT-60U [10]. Previous experiments on ITBs at JT-60U and other devices have pointed that modified toroidal rotation profiles, obtained by balancing neutral beam torques, affected ITBs [11-13]. It was shown that larger radial electric fields allowed the formation of stronger ITBs [14]. While JET operation with an enhanced TF ripple showed to have a significant impact on the toroidal rotation and rotational shear [15] which had an impact on the growth of ITBs [16, 17]. This paper will try to connect these earlier observations with the new experiments.

The experiments aimed to perform a dimensionless identity experiment on the formation and sustainement of internal transport barriers. This paper will first describe the experimental details in

section 2, discussing the scenarios used in JT-60U and JET to form ITBs. A satisfactory match of the main plasma parameters was achieved, while the differences that remained were exploited to study their impact on the transport barriers [18]. Section 3 will compare the main characteristics of the ITBs, as seen in both the JT-60U and JET experiments. Differences with respect to the q-profile development, the effect of the H-mode pedestal and the toroidal rotation profiles will be discussed. Section 4 will describe the impact of the toroidal rotation on the triggering and sustainement of ITBs. A summary of the observations and conclusions will be given in section 5 which also gives an outlook into future studies.

2. ITB EXPERIMENTS AT JT-60U AND JET

JT-60U and JET have roughly the same size and are therefore well suitable to carry out identity experiments. A near match to the shape of the magnetic configuration was achieved, as shown in figure 1. The elongation of the JET configuration was reduced from those used in standard operations, while the JT-60U configuration was moved inward to increase the inverse aspect ratio. The main characteristics of the configurations in JT-60U/JET were: an elongation of ^{o}=1.6/1.62, an triangularity of ´=0.23/0.22, while the inverse aspect ratio in JT-60U remained slightly lower with μ=0.24/0.29. The major and minor radii are R/a=3.4/0.8m and R=3.0/0.9m, for JT-60U and JET, respectively. The experiments were carried out at the same toroidal field (JT-60U/JET: B=2.26/2.25T) but the small differences in the shape, prevented a match of both the q95 and plasma current, Ip. Matching q95 at 4.2, the experiments in JT-60U had to use a lower plasma current of Ip=1.1MA compared to Ip=1.5MA at JET. It should be noted that these parameters are the same as, and hence allowing a direct comparison to, earlier JET ITB experiments reported in refs. [16, 17].

The average toroidal field ripple in JT-60U for these experiments was about ´BT=0.3%. JT-60U utilizes ferrite inserts to reduce its TF ripple, resulting in a rather complex TF ripple map and the value quoted here is an average found in the mid-plane at the separatrix. JET has the capability to operate at different TF ripple amplitudes and was operated with a TF ripple of ´BT=0.08%, the standard JET value, ´BT=0.3%, matching the JT-60U value and a higher value of ´BT=0.7% which affected the toroidal rotation [15].

The scenarios used to form ITBs were similar but not identical, as shown in figure 2. At JT-60U a constant current ramp rate of 0.5MA/s was used whereas at JET a slower ramp rate is used 0.3MA/s during most of the ramp-up phase. Both devices used early heating during the current ramp-up phase in order to tailor the q-profile, albeit this prelude heating was done by Neutral Beam Injection (NBI) in JT-60U, while JET used Lower Hybrid Current Drive (LHCD). The heating during the main experimental phase was supplied by NBI only with comparable power levels used in both JT-60U and JET. By adjusting the start time of the main heating, target q-profiles were obtained with either reversed magnetic shear (RS) in the centre (and a minimum q, qmin=3 or 2), or optimised low magnetic shear with q=2 in the centre. The tailoring of the q-profile is known to allow the triggering of ITBs. This paper will focus on the analysis of ITBs formed in RS plasmas only.

The experiments aimed to match the parameters at the time of ITB triggering. The details of the scenario to obtain this target may not be relevant to the ITB formation. Not all parameters may be matched perfectly and hence it is important to assess which are more relevant to ITBs and transport physics and matching should have a higher priority. One may argue that the shaping effects are less important for internal transport barriers than for example the pedestal comparison studies [7, 8]. As this is basically a transport comparison, it is evident that one should not merely have similar parameter quantities at one specific location in the plasma but match of the entire radial profile. Foremost of course the safety factor or q profile, which has shown to be of importance to ITBs, had to be the same, while also more weight was given to profiles of ¡*, Ω* (i.e. the normalised Larmor radius and collisionality) and the ratio of the electron and ion temperatures (Te/Ti) due to their relevance to transport physics, as discussed in ref. [18]. Moreover, the plasma rotation should be considered as it has been found previously to affect ITB physics in both devices.

A nice match of most relevant profiles was achieved in all cases, illustrated by the example shown in figure 3 for a JT-60U and JET case with qmin=3. In all cases the basic characteristic of the q-profile were matched but also the profiles of the dimensionless parameters ¡*, ≤tor-e and Ω* (where ≤ is the electron pressure normalised to the toroidal magnetic field pressure) were found to be near identical, as well as Te/Ti.

In order to match Ω* with a lower plasma current in JT-60U, it operated at lower density compared to JET. The density profile was also more peaked in JT-60U which is not fully understood. Furthermore, the toroidal rotation profiles did not match. The reason for this difference lies mainly with the details of the JT-60U and JET NBI systems. Although the injection energies are comparable, the injection angles and torque deposition profiles differ. In JET only co-current tangential injection can be applied whereas JT-60U has the capability to use injection normal to the plasma as well as both co and counter-current tangential NBI. This great flexibility allowed a torque scan at JT-60U, creating various toroidal rotation profiles. Similar experiments on ITBs were done previously (see ref. [12]) but the present rotation profiles differ significantly since ferrite inserts have been installed and the TF ripple was reduced at JT-60U [19]. It should be noted that even when the JET TF ripple amplitude was tuned to match that of JT-60U still no exact match in rotation profiles was obtained with the co-current only NBI.

3. COMPARING THE MAIN ITB CHARACTERISTICS.

Before comparing the observations in JT-60U and JET it is important to have a clear definition of an ITB. This can be done by a transport analysis, comparing the heat diffusivities in the ITBs or maybe more precise, studying the turbulence properties. Here at first a more practical approach has been applied comparing steepness of the temperature profile caused by the ITBs. The gradient can be expressed by a normalised value ¡*T”a¡s/LT, i.e the ratio of the ion Larmor radius at the sound speed and the temperature gradient length. This criterion has been applied successfully at JET to visualise the dynamic behaviour of ITBs [20]. A value of ¡*T>0.014 is the criterion used to identify

an ITB at JET. Here it will also be used on JT-60U data. The values in this paper are deduced for ion temperature profiles as measured by the Charge Exchange Spectroscopy (CXS) diagnostics.

In figure 4 the temporal behaviour of two ITB discharges from JT-60U and JET are shown. Both have a hollow target q-profiles with negative magnetic shear and qmin=3. The qprofile slowly evolves with the minimum q dropping to 2. The TF ripple was ´BT=0.3% and in both cases co-current NBI was applied resulting in a plasma rotating in co-direction, albeit slower in JT-60U. These examples show that the ITB behaviour can be rather dynamic and it is therefore not always easy to produce comparison overviews without losing information on this temporal behaviour.

The main ITB characteristics are remarkably similar. Firstly, ¡*T values are similar in both devices. Secondly, ITBs were initiated when qmin drops to a rational value. As reported before, these triggering events are characteristic for RS q-profiles in both devices [21, 22]. It should be noted that from Motional Stark Effect (MSE) measurements alone this moment cannot always been deduced accurately. However, it is often confirmed by the observation of Alfvén modes, called Alfvén cascades at JET [23] and reversed shear Alfvén eigenmodes (RSAE) at JT-60U [24]. In JET the earlier ITB, triggered by qmin=3, disappears at t=4s, likely due to the reduction of the reversed shear in the core, but a new ITB is triggered by the arrival of q=2. While in JT-60U the first ITB continues until the arrival of the q=2 surface, leading to a strengthening of the ITB. The position of the ITBs (i.e. location of maximum value ¡*T), roughly followed the location of the position of minimum q. The ITBs in JT-60U were found at a more outward radius, as the scenario used a faster current ramp-up, yielding a q-profile with a minimum q at larger radius.

Although the initial q-profiles were similar, the temporal evolution is not the same, leading to a different ITB behaviour. The global resistive time was found to be approximately the same yielding about fR=6s at the time of ITB triggering and fR=16s when the ITB was strongest. The difference in development of the q-profiles may be explained by the noninductively driven current profiles shown in figure 5a, calculated by the JETTO code [25]. In the first place, the NBI driven current fraction was larger at JET and predominantly on-axis causing the central negative shear region to degrade faster compared to JT-60U. Secondly, the fraction of bootstrap current was higher in JT-60U, mainly due to the lower plasma current, and hence higher poloidal ≤ (≤p), but also because of the more peaked density profiles in this device.

This causes the off-axis q or minimum q value in JT-60U to drop faster than in JET. The core current density in this JT-60U example actually decreases in time. For the examples shown in figure 4 the bootstrap and NBI driven current fractions were: 26% and 24% for JET and 68% and 21% for JT-60U, respectively. The importance of the non-inductive current profiles to the q-profile development and its impact on ITBs has already been pointed out in previous JT-60U studies [26].

A further contrast between the two cases shown in figure 4 is intermittent behaviour of the JET ITB triggered by q=3 while the JT-60U comparison case produces a more steady ITB. The ITB strength briefly diminishes from t=3.1-3.2s to reappear again after t=3.6s. This effect is connected to a transition in the pedestal, which suddenly increases the edge density as can be seen in figure 4b.

The H-mode pedestal density in JT-60U increases more smoothly. At JET this effect is often attributed to the impact of ELMs. Figure 4 shows, however, that the ELMs during the JET high pedestal density phase (t=3.0-3.5s), penetrate only slightly deeper than the milder ELMs in JT-60U and never reach the ITB. The ELM penetration does also not differ much from that found in JT-60U. Here the ELM penetration is defined as the most inner position where the effect on of the ELM crash on the temperature is less than 10% [27].

4. THE EFFECT OF PLASMA ROTATION

In order to study the impact of plasma rotation and rotational shear on ITBs, at JT-60U a series of discharges with identical target profiles but different plasma rotation were performed by balancing the NBI torque, while in JET the TF ripple was increased. In figure 6a a rough overview is given of the obtained maximum ITB strength and rotation properties of the various JET and JT-60U cases. Firstly, the dimensionless Mach number (MΔ), i.e. the plasma rotation normalised to the thermal velocity, is used to characterise the rotation. Clearly a larger variation in Mach numbers was obtained. JT-60U plasmas with pure co-NBI still had a lower rotation compared to JET with a similar TF ripple (´BT=0.3%). Only when the TF ripple amplitude was increased to ´BT=0.7-1% the JET central Mach number approached that found in JT-60U. As mentioned earlier the difference is due to the fact that the NBI deposition is not the same, possibly combined with differences in the TF ripple structure.

The Mach number may however not be the relevant parameter. In figure 6b the ITB strength is plotted versus the rotational shear, …ExB [2] (as calculated by the JETTO code, assuming neo-classical poloidal rotation). Similar values of rotational shear are found in JT-60U and JET, although in JET the dominant component is often due to the gradient in toroidal rotation, while in JT-60U other components like, the pressure gradient may contribute significantly to the radial electric field, especially in cases with near balanced NBI.

The figure shows that ITB are always triggered, independent of the rotational shear (1·104s-1<…ExB<2·104s-1) and weak ITBs (0.014<¡*T<0.023) can always be found in plasmas with reversed magnetic shear. This suggests that overall rotational shear, is not a dominant factor in the triggering of such these transport barriers.

But strong ITBs (¡*T>0.023) only develop to in JT-60U and JET plasmas that have sufficient rotational shear, i.e. …ExB>4-5·104s-1 in the vicinity of the ITB location. In figure 7 two JT-60U cases are compared; one with balanced NBI and the other with co-current NBI. For co- NBI the plasma rotates purely in co-current direction reaching angular rotation frequencies of 40krad/s (or a MΔ=0.28) in the centre, while for balanced NBI the outer part of the plasma rotates counter-current with a slow co-rotation in the core below 20krad/s (MΔ<0.1). The rotational shear at the time of ITB triggering was …ExB<2·104s-1 and …ExB=4·104s-1, respectively. A sudden growth and outward movement of the ITB is seen to start at t=6.8s for the case with pure co-NBI. The ITB strength reaches ¡*T=0.035 and further enhances the rotational shear to …ExB=7·104s-1 but is

terminated by the on-set of an MHD instability at t=7.18s. The q=2 surface appears in the plasma at t=6.2s as measured by MSE, with a hint of RSAE modes at the same time.

Previous experiments at JET have shown that when the rotational shear approaches the turbulence growth rate at the time an ITB is triggered, a non-linear growth process can start in which the barrier further increases the rotational shear and further quenches turbulence, yielding strong ITBs with ¡*T>>0.023 [17]. The JT-60U case with co-NBI, shows a very similar behaviour and the fast growth could have been initiated by the larger gradient in the rotation, seen to develop at t=6.2s. The rotational shear for these strong barriers indeed approaches the estimated growth rates of the Ion Temperature Gradient (ITG) mode growth rates in JET and JT-60U. More detailed modelling of the turbulence growth rate is needed to get a clearer understanding of the impact of rotational shear on the growth of these strong ITBs and how they differ from the weaker ITBs.

CONCLUSIONS

The identity experiments presented in this paper aimed to find common characteristics of transport barriers in both JT-60U and JET, which would help to find a more established understanding of ITBs. When a proper match is achieved of the most relevant profiles, very similar ITB characteristics were observed in JT-60U and JET, suggesting that they were governed by the same physics.

The match was achieved at the time of ITB triggering. In this case both in JT-60U and JET similar ITBs were triggered by the minimum q value decreasing below and integer value. The q-profile plays a dominant role in this process while the mechanism seems to be independent of the toroidal plasma rotation or rotational shear, as was also found in earlier JET experiments [17]. After triggering, ITBs of similar strength were observed. Here the ¡*T parameter was used to compare ITB strength and comparable values are to be expected as both devices seem to have the same values for ¡s and temperature profiles. It should be noted though, that earlier analysis has shown that this parameter may not necessarily scale to other the devices [29].

Differences in the further development of the ITBs remained due to variations in the qprofile development, the H-mode pedestal pressure and the plasma rotation. In JT-60U a larger non-inductive current fraction was driven off-axis, allowing it to keep the reversed magnetic shear longer, which was beneficial for these ITBs. This again indicates the importance of the q profile control and the alignment of non-inductively driven current profile with respect to the ITB sustainement [6, 26].

The characteristic higher H-mode pedestal pressure influenced the ITB in JET. Increasing the TF ripple in JET (up to ´BT=0.7%) did not affect the pedestal and ELMs sufficiently to reduce its influence on the ITB. This common feature in JET is often attributed to ELMs. These experiments suggest that the effect could however be more complex, involving the underlying plasma turbulence and profile stiffness, and more studies are needed to obtain a full understanding. This is especially relevant for operation at higher triangularity, which often results in a more pronounced H-mode, complicating the formation of ITBs [30]. Though, recent efforts at JET resulted in the development of a high triangularity Advanced Tokamak scenario with ITBs [31].

The toroidal rotation was varied in these experiments, allowing an investigation into the role of plasma rotation and rotational shear on the development of ITBs. As said above, this did not have any impact on the triggering of ITBs in reversed magnetic shear, but their further development was affected. Usually the ITBs were found to be of moderate strength (¡*T<0.023) but when sufficient co-current NBI was applied at JT-60U fast growing ITBs were observed.The difference between weak and strong ITBs in JT-60U and its connection with plasma rotation has been reported before [12]. It is also identical to the observations in previous JET experiments which showed that these strongly growing ITBs could be prevented by increasing the TF ripple and reducing the rotational shear [16, 17]. In contrast to the weaker ITBs, the impact of these ITBs on the momentum confinement, further enhancing the rotational shear and suppressing turbulence, may result in a non-linear growth of the barrier [17]. Strong ITBs could provide an ideal confinement for an Advance Tokamak scenario. But the un-controlled growth and steep gradients often lead to stability problems that either destroy the ITB or even cause a disruption of the discharge.

This paper gives a first overview of the observations from these experiments. The comparison of the observations revealed strong similarities between the physics of ITBs formed in JT-60U and JET. The main ingredients for their sustainement, such as the q-profile development and rotational shear need to be controlled if ITBs are to be utilized successfully in Advanced Tokamak scenarios. Further efforts are being undertaken, using an identical set of modelling tools, to study the transport properties and associated turbulence in these discharges, which will be the subject of future reports.

ACKNOWLEDGEMENT

The experiments have been carried out under the patronage of the ITPA and in the frameworks of the IEA Large Tokamak and European Fusion Development Agreements. The research was funded partly by the UK EPSRC and by the European Communities under the contract of Association between EURATOM, UKAEA and CEA. The views and opinions expressed herein do not necessarily reflect those of the European Commission.

REFERENCES

[1]. J.W. Connor, et al. 2004 *Nuclear Fusion* **44** R1.
[2]. K.H. Burrell, et al. 1997 *Phys. Plasmas* **4** 1499.
[3]. M. Kikuchi, et al. 1990 *Nuclear Fusion* **30** 265.
[4]. T.C. Luce, et al. 2003 *Nuclear Fusion* **43** 321.
[5]. X. Litaudon, et al. 2002 *Plasma Physics Controlled Fusion* **44** 1057.
[6]. C.D. Challis, 2004 *Plasma Physics Controlled Fusion* **46** 2004.
[7]. G. Saibene, et al., 2007 *Nuclear Fusion* **47** 969.
[8]. N. Oyama, et al. 2008 *J. Phys.: Conf. Ser.* **123** 012015.
[9]. M. Becoulet, et al. 2003 *Plasma Physics Controlled Fusion* **45** A93.
[10]. Y. Kamada, et al., 2006 *Plasma Physics Controlled Fusion* **48** A419.

[11]. H. Shirai, et al. 2000 *Plasma Physics Controlled Fusion* **42** A109.
[12]. Y. Sakamoto, et al. 2001 *Nuclear Fusion* **41** 865.
[13]. E.J. Synakowski, et al. 1997 *Physical Review Letters* **78** 2972.
[14]. Y Sakamoto, et al. 2004 *Nuclear Fusion* **44** 876.
[15]. P.C. de Vries, et al. 2008 *Nuclear Fusion* **48** 035007.
[16]. P.C. de Vries, et al. 2008 *Plasma Physics Controlled Fusion* **50** 065008.
[17]. P.C. de Vries, et al. 2009 *Nucl. Fusion* **49** 075007.
[18]. T.C. Luce, C.C. Petty, J.C. Cordey, 2008 *Plasma Physics Controlled Fusion* **50** 043001.
[19]. M. Yoshida, et al. 2006 *Plasma Physics Controlled Fusion* **48** 1673.
[20]. G. Tresset, et al., 2002 *Nuclear Fusion* **42** 520.
[21]. S.V. Neudatchin, et al., 2004 *Nuclear Fusion* **44** 945.
[22]. E. Joffrin, et al., 2003 *Nuclear Fusion* **43** 1167.
[23]. S.E. Sharapov, et al. 2001 *Phys Lett. A* **289** 137.
[24]. H. Kimura, et al. 1998 *Nuclear Fusion* **38** 1303.
[25]. G. Cenacchi and A Taroni, 1986 in Proc. 8th Computational Physics, Computing in Plasma Physics (Petit-Lancy, 1986) (Geneva: European Physical Society) Vol. 10D p57
[26]. S. Ide, et al. 2002 *Plasma Physics Controlled Fusion* **44** L63.
[27]. M.N.A Beurskens, et al. 2008 *Nuclear Fusion* **48** 095004.
[28]. Y Kamada et al. in Fusion Energy 2008 (Proc. 22nd Int. Conf. Geneva, 2008) (Vienna: IAEA) CD-ROM file EX/P3-3 and http://www-naweb.iaea.org/napc/physics/FEC/FEC2008/html/index.htm
[29]. T. Fujita, et al., in Proc. 30th EPS Conf. on Control. Fusion and Plasma Phys. (St. Petersburg, 2003) ECA Vol. 27A, P-2.131 and http://epsppd.epfl.ch/StPetersburg/PDF/P2_131.PDF
[30]. F.G. Rimini, et al. 2005 Nuclear Fusion **45** 1581.
[31]. J. Mailloux, et al. "Development of a steady-state scenario in JET with dimensionless parameters approaching ITER target values" in the Proc. 36th EPS Conf. on Plasma Phys. (Sofia, 2009).

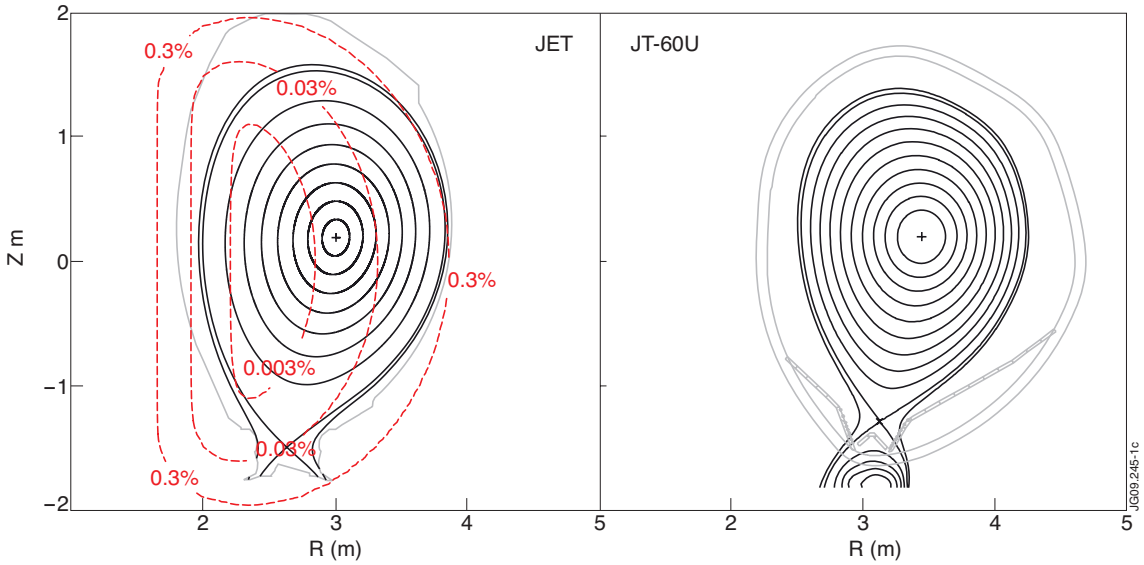

Figure 1: Comparison of the plasma shape in JET (left) and JT-60U (right) as used in these experiments. The JET TF ripple contours for a case which matches the average JT-60U TF ripple at the separatrix are shown.

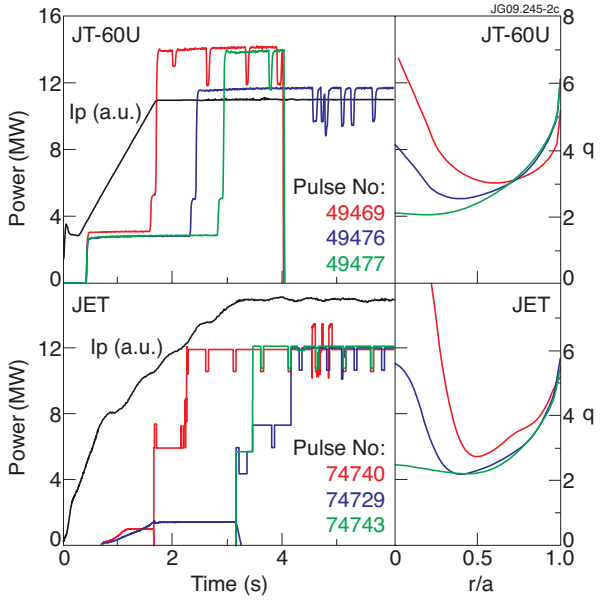

Figure 2: A comparison of the three main heating scenarios, used for these experiments at JT-60U (top) and JET (bottom). The plasma current waveforms (in units 100kA) for both devices are given in black on the left. By altering the prelude heating (during the current ramp-up) and retiming the start of the main heating phase, three different target q-profiles, as measured by the MSE diagnostic, were produced at the start of the main heating phase (i.e. start of maximum power). These are shown as function of normalised radius on the right. The JT-60U used low power NBI as prelude, while in the JET Pulse No: 74740 and 74729, a prelude of LHCD was applied.

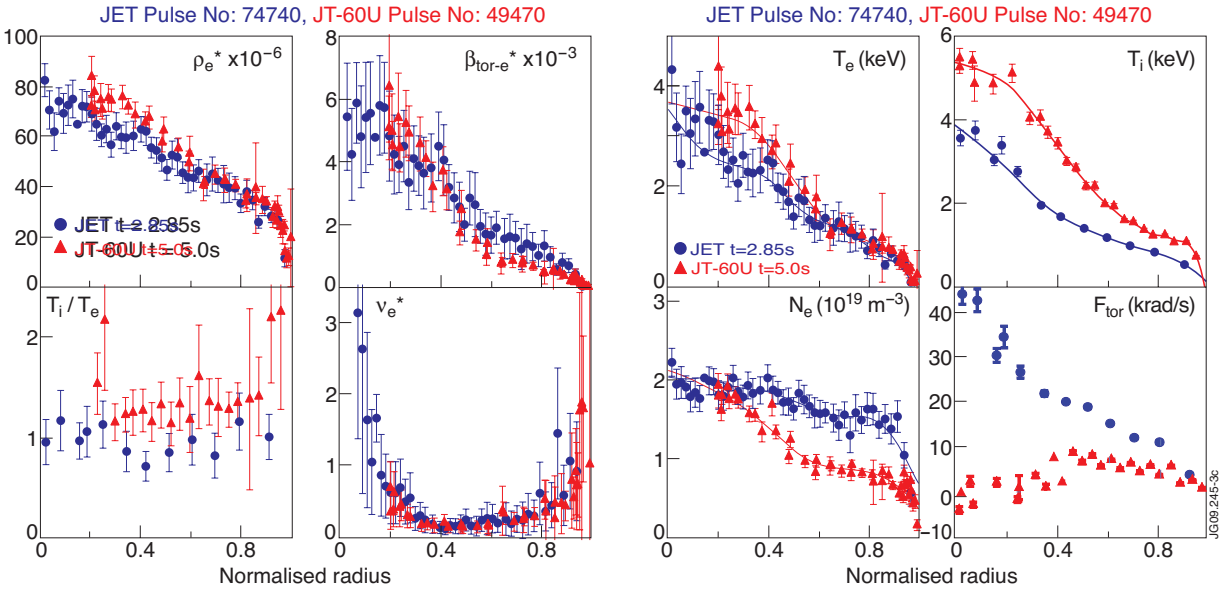

Figure 3: Example of parameter matching, showing the profiles for two comparison cases, both with the same TF ripple (0.3%), at the time of ITB triggering with a q profile with negative shear and $q_{min} = 3$. On the left the profiles of the dimensionless parameters, ρ, β and T_e/T_i and ν*, respectively. On the right the electron (T_e) and ion (T_i) temperature profiles, together with those for the electron density (ne) and toroidal angular rotation frequency.*

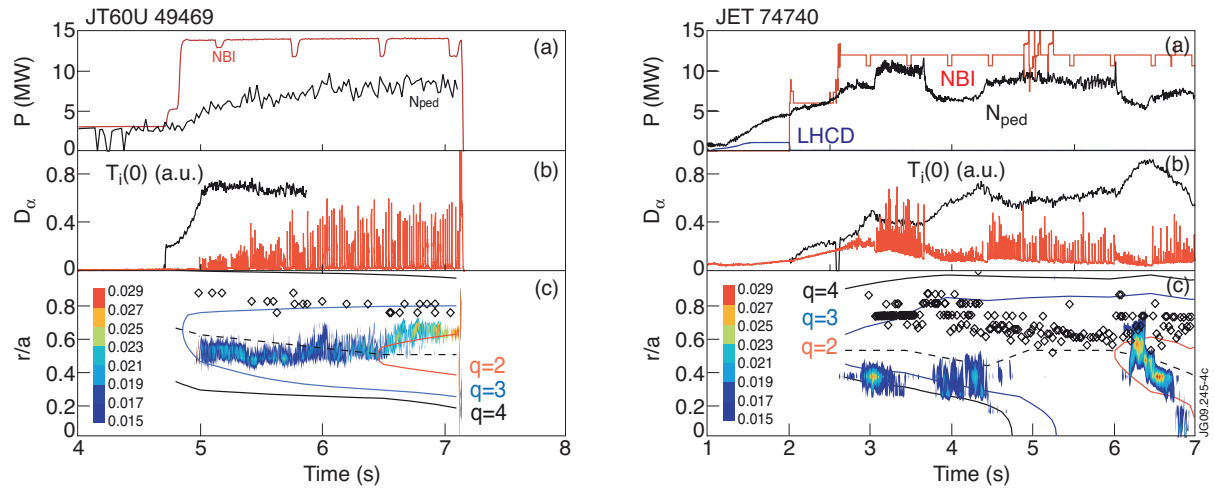

Figure 4: On the left a typical JT-60U case with co-NBI and on the right a JET case with TF ripple of $\delta_{BT} = 0.3\%$. Both with co-current NBI and a target q-profile with RS and q_{min}=3 at t=2.8s and t=4.9s, respectively. a) The heating (LHCD, NBI) time traces, with in black the pedestal density (a.u.). b) The D_α signal together with the central ion temperature. c) A contour plot showing the values of ρ^*_T as a function of time and the normalised radius. Overlaid by the contours of q = 4, 3 and 2, showing the behaviour of the q-profile, as measured by MSE. The position of the minimum q is given by the dashed curve. The diamonds give the 'ELM penetration', i.e. the position where the effect of the ELM on the temperature is less than 10%.

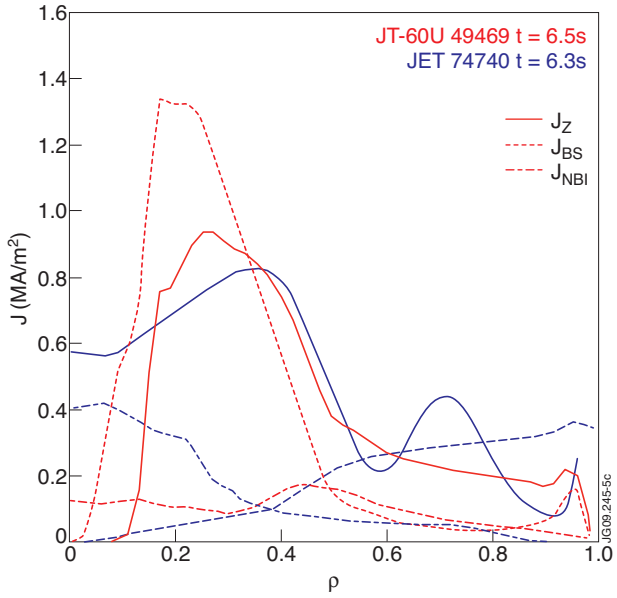

Figure 5: a) The NBI driven current (dot dashes) and Bootstrap current (dashed) and total current density (solid line) profiles for the JET(blue) and JT-60U (red) examples shown in figure 4. These have been calculated using the JETTO code [25].

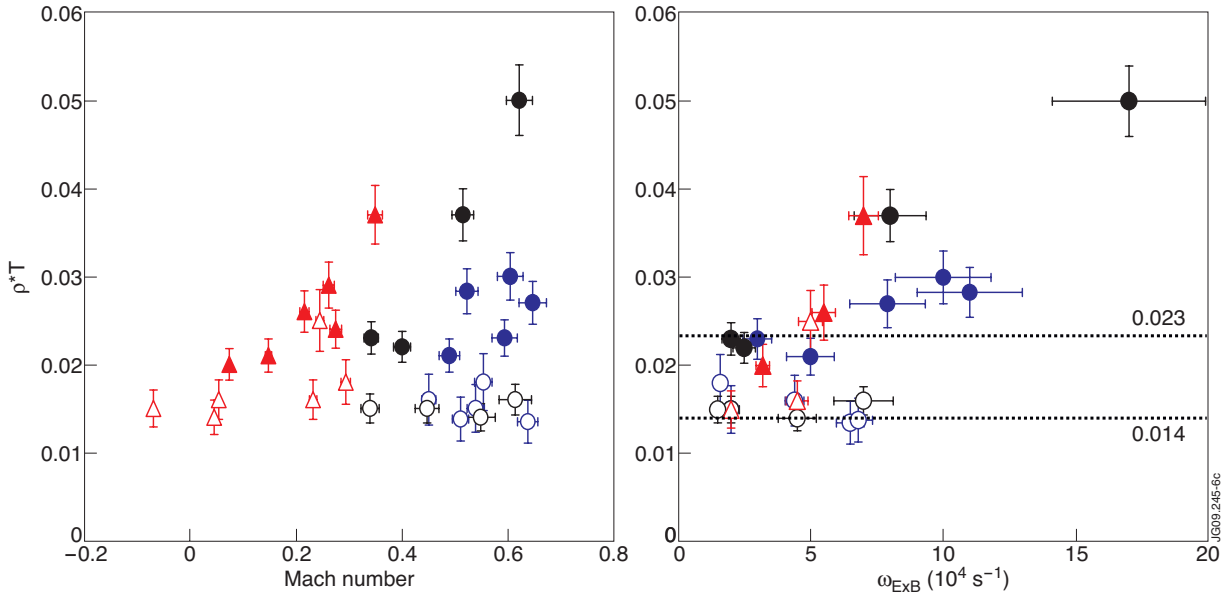

*Figure 6: a) The value of ρ*Ti plotted versus the central Mach number for various JT-60U (red triangles) and JET (black/blue dots) cases. The open symbols show the values at the time the ITB is triggered, while the close symbols are at the time of maximum ITB strength. b) The same data but plotted versus the rotational shear, $\omega_{E\times B}$ in the vicinity of the ITB.*

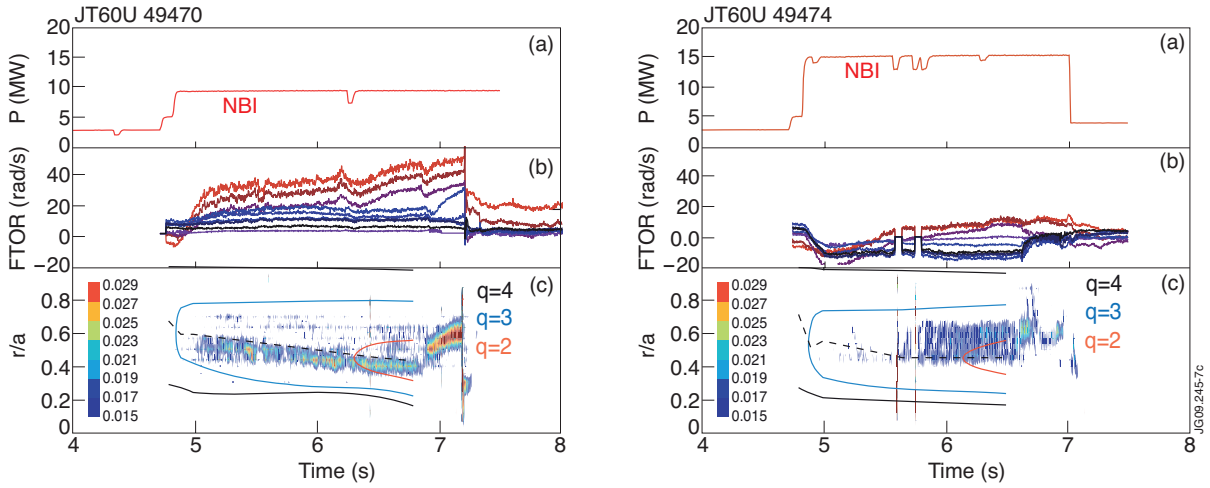

Figure 7: Two JT-60U discharges with pure co-NBI (left: Pulse No: 49470) and balanced NBI (right: Pulse No: 49474) showing a) The NBI power b) the 9 time traces of the rotation at r/a=0.1, 0.2, 0.3, 0.4, 0.5, 0.6, 0.7, 0.8 and 0.9 (coloured from red, to blue, respectively) c) A contour plot showing the values of ρ^*_T as a function of time and the normalised radius. Overlaid by the contours of q = 4, 3 and 2, showing the behaviour of the q-profile, as measured by MSE. The position of the minimum q is given by the dashed curve.